Pergamon

Geochimica et Cosmochimica Acta, Vol. 68, No. 2, pp. 387–401, 2004

0016-7037/04 $30.00 + .00

doi:10.1016/S0016-7037(03)00484-8

Solubilities of nitrogen and noble gases in silicate melts under various oxygen fugacities: Implications for the origin and degassing history of nitrogen and noble gases in the Earth

AKIKO MIYAZAKI,[1,*] HAJIME HIYAGON,[1] NAOJI SUGIURA,[1] KEI HIROSE,[2] and EIICHI TAKAHASHI[2]

[1]Department of Earth and Planetary Science, Graduate School of Science, University of Tokyo, Hongo 7-3-1, Bunkyo-ku, Tokyo 113-0033, Japan

[2]Department of Earth and Planetary Science, Graduate School of Science and Technology, Tokyo Institute of Technology, Ookayama 2-12-1, Meguro-ku, Tokyo 152-8551, Japan

(*Received March* 11, 2003; *accepted in revised form July* 9, 2003)

Abstract—Solubility experiments for nitrogen and noble gases (Ar and Ne) in silicate melts were conducted using two experimental configurations: one was conducted at 1 atmospheric pressure, $T = 1300$°C and oxygen fugacity (fO_2) of IW + 0.9 (i.e., 0.9 log units higher than the iron-wüstite buffer) and the other at high pressures ($P_{total} \sim 2 \times 10^8$ Pa), 1500°C and $fO_2 \sim$ IW + 6. For the former experiment, isotopically labeled-nitrogen ($^{15}N^{15}N$-enriched) was used to distinguish dissolved nitrogen from contaminating atmospheric or organic nitrogen and to examine dissolution mechanisms of nitrogen in silicate melts. The results obtained for the two series of experiments are consistent with each other, suggesting that Henry's law is satisfied for fN_2 of up to ~250 atm (2.5×10^7 Pa). The results are also consistent with our earlier results (Miyazaki et al., 1995) obtained at highly oxidizing conditions ($fO_2 \sim$ IW + 10). All these results support physical dissolution of nitrogen as N_2 molecules in silicate melts for fO_2 from ~IW + 10 down to ~IW. The observed solubility (Henry's constant) of nitrogen ($3–5 \times 10^{-9}$ mol/g/atm) is comparable to that of Ar ($2–4 \times 10^{-9}$ mol/g/atm), and much lower than that of Ne ($11–14 \times 10^{-9}$ mol/g/atm) at 1300°C. A preliminary experiment was also performed for partitioning of nitrogen and noble gases between clinopyroxene (cpx) and basaltic melt using a piston cylinder-type apparatus at 1.5 GPa and at 1270 to 1350°C. The obtained cpx/melt partition coefficient of nitrogen is 0.06, slightly lower than those of noble gases (~0.1 for Ne to Xe), suggesting that nitrogen is as incompatible as or even slightly more incompatible than noble gases. The present results imply that a large nitrogen/Ar fractionation would not be produced by magmatic processes. Therefore, the two orders of magnitude difference between the $N_2/^{36}Ar$ ratios in the Earth's atmosphere (~10^4) and that in the mantle (~10^6) must be explained by some other processes, such as incomplete segregation of metal blobs into the core and their later oxidation.

1. INTRODUCTION

Nitrogen is a major constituent of the Earth's atmosphere, but its degassing history is poorly known. Degassing of volatile elements from the Earth's interior may have been in large part driven by magmatic processes, in which solid/melt and melt/gas partitioning have played important roles. However, our knowledge about partitioning of nitrogen is very limited.

If nitrogen has a degassing history very similar to that of noble gases, the present $N_2/^{36}Ar$ ratios in the atmosphere and in the mantle must be very similar to each other. However, there is two orders of magnitude difference in the $N_2/^{36}Ar$ ratio between the atmosphere (~10^4) and the mantle (>10^6; estimated from submarine glasses) (Marty, 1995; Miyazaki, 1996). This may be understood by the difference in degassing efficiency of N_2 and ^{36}Ar from the Earth's interior to the atmosphere and/or preferential transport of nitrogen from the surface reservoirs (atmosphere + sediments) back to the mantle. Marty et al. (1996) proposed that preferential retention of nitrogen in the mantle might occur under reducing conditions in the early history of the Earth, which resulted in the higher $N_2/^{36}Ar$ ratio in the mantle. To examine such a possibility and to better understand the degassing history of nitrogen, it is essential to study partitioning of nitrogen in the gas-melt, melt-solid and metal-silicate systems.

Melt/gas partition coefficients, or solubilities, of noble gases in silicate melts were reported by many authors; it is well documented that (1) they satisfy Henry's law (up to a few kilobar, or a few hundred million pascals), (2) they decrease with increasing molecular diameter in the order of He, Ne, Ar, Kr and Xe, (3) they increase slightly with increasing temperature and (4) they depend on the melt compositions (e.g., Kirsten, 1968; Hayatsu and Waboso, 1985; Hiyagon and Ozima, 1986; Jambon et al., 1986; Lux, 1987; White et al., 1989; Broadhurst et al., 1990, 1992; Carroll and Stolper, 1993; Montana et al., 1993; Shibata et al., 1994, 1996, 1998; Chamorro-Pérez et al., 1996, 1998; Schmidt and Keppler, 2002; Kelly, 2002).

On the other hand, there is only limited work on the solubility of nitrogen in silicate melts having compositions of geological interest. The solubility of nitrogen under highly oxidizing conditions (fO_2 = IW + 6 to IW + 10, i.e., 6–10 log units higher than IW, where IW represents iron-wüstite buffer) was measured at 1600°C by Marty et al. (1995) and at 1300°C by Miyazaki et al. (1995), and found to be almost comparable to that of argon. Fogel (1994) measured the solubility of nitrogen in a synthetic melt (an FeO-, K_2O-, Na_2O- and TiO_2-free 1921 Kilauea basalt composition, simulating aubrite or E-chondritic melts) at 1500 to 1600°C under highly reducing

* Author to whom correspondence should be addressed (amiya@eps.s.u-tokyo.ac.jp).

conditions ($fO_2 \sim$ IW $-$ 10). The obtained solubilities are five orders of magnitude higher than those obtained at oxidizing conditions. This suggests that solubility of nitrogen is highly dependent on oxygen fugacity, but there are no data for the oxygen fugacity corresponding to the mantle condition except for recent preliminary works by Miyazaki (1996) and Humbert (1998). The oxidation state of the present mantle is estimated to be within 1 to 2 log units of fayalite-magnetite-quartz (FMQ) buffer, based on the Fe^{3+}/Fe^{2+} ratios of quenched Mid-Ocean Ridge Basalt (MORB) glasses (Christie et al., 1986) and based on the oxidation state of iron in spinel lherzolites and pyroxenites measured with ^{57}Fe Mössbauer spectroscopy (Wood and Virgo, 1989; Canil et al., 1994). The mantle may have been more reducing (~IW) when it coexisted with metals, which eventually segregated from the mantle to form the core (e.g., Arculus, 1985; Kuramoto and Matsui, 1996). Therefore, solubility of nitrogen in silicate melts under the oxygen fugacity from IW to FMQ would have special importance in Earth sciences.

In the present study, we conducted solubility experiments for nitrogen and noble gases (Ar and Ne) in silicate melts (mostly of basaltic composition) under moderately reducing conditions (down to ~IW). In the experiments performed at one atmospheric pressure, we used a $^{15}N^{15}N$-labeled gas for (1) eliminating the effect of atmospheric contamination in the analysis and (2) understanding the dissolution mechanism of nitrogen by monitoring the presence or absence of isotopic exchange between nitrogen molecules during sample synthesis (Miyazaki et al., 1995).

So far, no data are available for solid/melt partitioning of nitrogen while several works for noble gases have been reported (Hiyagon and Ozima, 1986; Broadhurst et al., 1990, 1992; Brooker et al., 1998; Chamorro et al., 2002; Kelly, 2002). We synthesized a clinopyroxene (cpx)-basaltic melt pair using a piston-cylinder-type apparatus at 15 kbar at 1270°C, and measured the partition coefficients of nitrogen and noble gases between cpx and melt. Although the results are still preliminary, they would give valuable information about the behavior of nitrogen in magmatic processes.

2. MATERIAL AND METHODS

2.1. Solubility Experiments

Two types of apparatus were used for the solubility experiments: an electric furnace operated at one atmospheric pressure, in which oxygen fugacity was controlled by changing the flow rate of CO/CO_2 (fO_2-controlled experiments) and a gas-medium high pressure apparatus, in which high partial pressures of nitrogen and noble gases were applied ($P_{total} \sim 2 \times 10^8$ Pa) (high pressure experiments).

2.2. fO_2-Controlled Experiments (L-series)

A degassed basaltic glass (DB), synthesized under high vacuum, and a $^{15}N^{15}N$-enriched basaltic glass (EB; containing 19.7×10^{-12} mol/g of $^{15}N^{15}N$), synthesized by melting DB under an atmosphere enriched in $^{15}N^{15}N$ by 1700 times normal air, were used for the starting materials. The DB and the EB glasses were cut into thin plates (~0.8 mm thick) and were placed (~400 mg) on a piece of platinum mesh (an 80-mesh and 0.08 mm in diameter). The glasses were melted in an electric furnace at 1300°C in a flowing gas mixture of Ar, Ne, $^{15}N^{15}N$-labeled nitrogen and CO_2 + CO with a total flow rate of ~10 cm^3/s (Fig. 1). The $^{15}N^{15}N$-labeled nitrogen (prepared by Takachiho Trading Co., Ltd., Tokyo) was a mixture of atmospheric nitrogen and a $^{15}N^{15}N$ gas, with $^{15}N^{15}N$ concentration of 290 times higher than that in the normal air. The oxygen fugacity (fO_2) was kept at IW + 0.9 by controlling the flow rate of CO/CO_2. The sample formed a thin melt layer on the platinum mesh, which could be equilibrated with the ambient gas in a short time. After 0.3 to 4.5 h of heating, the melt was quenched in the gas flow by dropping it to the bottom of the reaction tube. The run products started with DB and EB must give identical solubilities if equilibrium was attained in the present experimental conditions. Chemical compositions of the starting materials and the experimental conditions are summarized in Tables 1 and 2a, respectively.

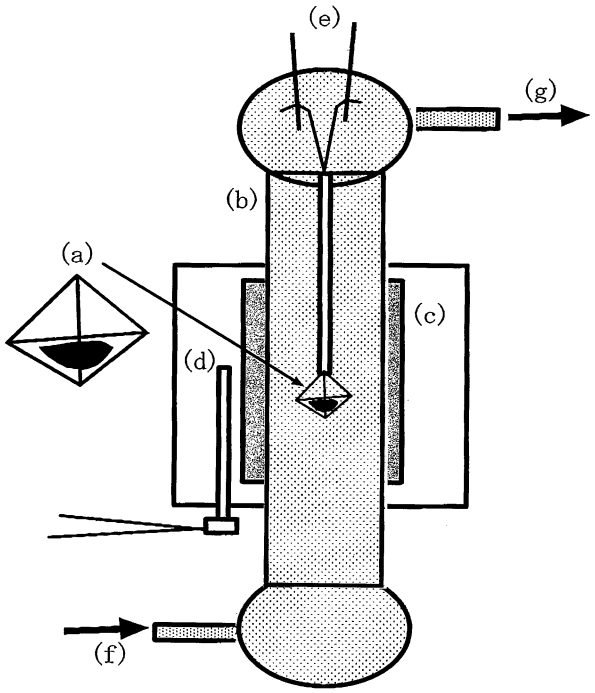

Fig. 1. A schematic diagram of the electric furnace used for the fO_2-controlled (L-series) experiments: (a) a tetrahedral ceramic framework holding thin glass plates (~0.8 mm thick) on a Pt-mesh, (b) alumina cylinder (35 mm in diameter, ~1 m in length), (c) SiC heater, (d) thermocouple, (e) electric terminals for sample quench, (f) and (g) gas flow.

In our earlier experiments (Miyazaki, 1996), we used less $^{15}N^{15}N$-enriched nitrogen ($^{15}N^{15}N$ concentration of 46 times air) and conducted the solubility experiments for wider range of fO_2 (from IW + 4 down to IW $-$ 1, controlled by changing the flow rate of CO/CO_2 or H_2/CO_2) at different temperatures (1200–1600°C). The results, however, have larger uncertainties due to lower concentration of the recovered excess ^{15}N and unstable conditions of the quadrupole-type mass spectrometer. Although there is overall consistency between the two sets of data, we present here only our newer results.

Table 1. Chemical compositions of the starting materials (wt%).

	DB[a]	AND[b]	DA[c]
SiO_2	53.56	57.22	50.7
TiO_2	1.04		
Al_2O_3	14.70	17.46	13.2
Fe_2O_3	11.65	2.45	
FeO		6.15	
MnO	0.00	0.16	
MgO	5.45	3.77	11.9
CaO	9.33	7.93	23.8
Na_2O	2.43	2.87	
K_2O	0.53	0.31	
P_2O_5		0.10	
Total	98.68	100.13	100.0

[a] Degassed basalt glass: synthesized from powdered basalt collected at Izu-Oshima, Japan. (Analyzed with EPMA.)
[b] Andesite collected at Hakone-toge, Japan (Kuno, 1935).
[c] Synthetic glass powder: a mixture of 64% diopside and 36% anorthite. (Calculated composition.)

2.3. High-Pressure Experiments (H-series)

Since oxygen fugacity could not be controlled in the gas-medium high pressure apparatus, we prepared Fe(III)/Fe(II) ratio-regulated glasses (BFa, BF7 and BF11) as starting materials to see if fO_2 of the starting material could cause any difference in nitrogen solubility. Basalt powder was melted completely at 1270°C for a few hours in air (BFa), or in the flowing $H_2 + CO_2$ gases so that fO_2 was controlled to be $\sim 4 \times 10^{-7}$ atm ($\sim 4 \times 10^{-2}$ Pa) (BF7) or $\sim 1 \times 10^{-11}$ atm ($\sim 1 \times 10^{-6}$ Pa) (BF11). The Fe(III)/Fe(II) ratios of BFa, BF7 and BF11 were estimated to be 1.92, 0.33 and 0.04, respectively, using ^{57}Fe Mössbauer spectrometry. However, the run products started with these three glasses showed almost identical Fe(III)/Fe(II) ratios corresponding to $fO_2 \sim$ IW + 6. An FeO-enriched glass (BFI; 90 wt.% basalt + 10 wt.% hematite, synthesized at 1270°C under $fO_2 \sim 1 \times 10^{-11}$ atm or 1×10^{-6} Pa), a $Di_{64}An_{36}$ glass (DA; 64 wt.% diopside + 36 wt.% anorthite) and andesite powder (AND) were also used for the starting materials to examine dependence on chemical compositions. Chemical compositions of the starting materials are listed in Table 1.

The starting materials were powdered (≤ 150 μm in size) and were put (60–100 mg) in Pt-capsules (3 mm in diameter, ~10 mm in length). The top of the capsule was only loosely pinched so that the mixed gas of nitrogen and noble gases could be freely exchanged between inside and outside of the capsules. Several samples thus prepared were put together in a Mo-basket, suspended in the pressure vessel of the gas-medium high-pressure apparatus (SMC-2000; the furnace assembly is shown in Miyagi, 1995), and heated with a Mo-heater up to 1500°C under the atmosphere of ~2000 bar (~0.2 GPa) of N_2 + Ar. The samples were melted in the Pt-capsules for 2 h to equilibrate with the ambient gas and quenched. Oxygen fugacity in the vessel was estimated to be $fO_2 \sim$ IW + 6 based on the Fe(III)/Fe(II) ratios of the run products measured with a ^{57}Fe Mössbauer technique. The experimental conditions are summarized in Table 2b.

In our earlier experiments (Miyazaki, 1996), we also used chipped glasses (a few millimeters in diameter) for the starting materials. However, the results show consistently lower solubility for nitrogen. We suspect solubility equilibrium was not fully attained for these samples. For this reason and for unstable conditions of the mass spectrometer during the earlier experiments, we present here only our recent results.

2.4. Gas Analysis

The run products (both L- and H-series) were gently crushed and removed from Pt-mesh or Pt-capsules. Almost all the sample was recovered. About 10 to 90 mg of them was wrapped in Pt-foil, loaded in a vacuum line for gas extraction. A stepwise combustion method was employed to distinguish dissolved nitrogen and noble gases (Ar and Ne) in the sample from atmospheric and organic (nitrogen) contaminations. The samples were heated in a quartz reaction tube under 80 to 260 Pa of oxygen from 400 to 1200°C with 100 to 200°C intervals with 25 min for each step. After the 1200°C step, L-18 and L-19 showed swollen Pt packages. They were put in a crushing vessel connected to the extraction line and the gases remaining in the capsules were analyzed, but they turned out to be negligible. All the L-series samples were further combusted using Nd-YAG laser under 30 to 60 Pa of oxygen, first at ~1100°C to remove atmospheric contamination and then at ~1800°C to melt the samples completely.

The purification procedure of the extracted gas was essentially the same as described in Hashizume and Sugiura (1990). The extracted gas was first exposed to hot CuO (760°C, O_2 pressure of ~30 Pa) to oxidize CO and hydrocarbons and then to Cu-CuO (630°C and then cooled to 400°C) to adsorb the remaining oxygen. Contaminating gases (CO_2, H_2O, etc.) were removed using glass cold traps (cooled with liquid nitrogen). About half of the purified gas was used for the nitrogen analysis; the rest of the gas was first exposed to hot Ti (~300°C) to remove nitrogen and to another cold trap (stainless filters

Table 2a. Experimental conditions for the fO_2-controlled solubility experiments conducted at 1 atmospheric pressure.

Run #	Temp. (°C)	Time (h)	Starting material	Gas flow rate (cm^3/s) Total	CO_2	CO	log(fO_2) (atm)	$P(^{14}N^{14}N)$ (atm)	P(excess $^{15}N^{15}N$), (atm)	$P(^{40}Ar)$ (atm)	$P(^{20}Ne)$ (atm)
L-14	1300	0.33	DB	8.1	2.0	2.0	−9.91	0.460	0.00169	0.0521	0.00049
L-15	1300	1	DB	8.1	2.0	2.0	−9.91	0.460	0.00169	0.0521	0.00049
L-16	1300	2.5	DB	8.1	2.0	2.0	−9.91	0.460	0.00169	0.0521	0.00049
L-17	1300	4.5	DB	8.1	2.0	2.0	−9.91	0.460	0.00169	0.0521	0.00049
L-18	1300	1	EB	8.1	2.0	2.0	−9.91	0.460	0.00169	0.0521	0.00049
L-19	1300	4.5	EB	8.1	2.0	2.0	−9.91	0.460	0.00169	0.0521	0.00049

Table 2b. Experimental conditions for the solubility experiments using a gas-media high pressure vessel.

Run #	Temp. (°C)	Time (h)	Starting material	$P(N_2)$ (atm)	P(Ar) (atm)	P(Ne) (atm)	$f(N_2)$ (atm)	f(Ar) (atm)	f(Ne) (atm)	$\log(fO_2)$ (atm)
H-9	1500	2	AND	157	1858	0.0	247	2671	0.0	–2.66
H-10	1500	2	BFa, BF7, BF11 BFI, DA	140	1730	0.0	212	2429	0.0	–2.85

cooled with liquid nitrogen) to separate Ne and Ar. Nitrogen, Ne and Ar fractions thus separated were successively analyzed with a quadrupole-type mass spectrometer (MSQ-400, ULVAC Co.).

In the nitrogen measurement, masses (m/e) of 28, 29, 30 and 26 were analyzed repeatedly for 20 cycles. Mass 26 was used for monitoring and correcting hydrocarbons in the mass range of 28 to 30. Interfering species of CO and hydrocarbons were numerically subtracted from the results. For L-series samples synthesized under the $^{15}N^{15}N$-labeled gas, however, contribution of CO was not corrected because of difficulties in its estimation, but the contribution of CO and hydrocarbons seem to be negligible for most of the samples judging from the intensity of mass 31 ($^{13}C^{18}O$ + hydrocarbon), which was monitored at the end of the analysis.

In the argon measurement, masses (m/e) of 36, 38 and 40 were analyzed repeatedly for 20 cycles.

In the neon measurement, masses (m/e) of 18, 20, 21, 22, 40 and 44 were analyzed repeatedly for 20 cycles. Mass 18 was used for monitoring and correcting water (H_2O) in the mass range of 20 to 22, which was found to be very low. Mass 40 and 44 were used for the correction of doubly charged ^{40}Ar ($^{40}Ar^{2+}$) to $^{20}Ne^{+}$ and $^{44}CO_2{}^{2+}$ to $^{22}Ne^{+}$, respectively. The production ratios of $^{40}Ar^{2+}/^{40}Ar^{+}$ and $^{44}CO_2{}^{2+}/^{44}CO_2{}^{+}$ were 6.05 and 0.54%, respectively, in our system. The amount of correction for ^{20}Ne was only $< 0.2\%$, since almost all argon was removed from the sample gas before the Ne analysis and the intensity of mass 40 was much lower than mass 20 between 400 and 800°C fractions, at which most of Ne was released from the sample.

From the measured concentrations of nitrogen and noble gases in the samples and their partial pressures in the ambient gas phase during the sample synthesis, we calculated the solubilities (melt/gas partition coefficients) of the gases. For the L-series samples, we used excess ^{15}N instead of total nitrogen for the solubility calculations. Excess ^{15}N is defined as follows:

$$Excess\ ^{15}N\ in\ mass\ 29 = \left\{ \left(\frac{^{14}N^{15}N}{^{14}N^{14}N} \right)_{obs} - \left(\frac{^{14}N^{15}N}{^{14}N^{14}N} \right)_{air} \right\} \times [^{14}N^{14}N]_{obs} \quad (1)$$

$$Excess\ ^{15}N\ in\ mass\ 30 = \left\{ \left(\frac{^{15}N^{15}N}{^{14}N^{14}N} \right)_{obs} - \left(\frac{^{15}N^{15}N}{^{14}N^{14}N} \right)_{air} \right\} \times [^{14}N^{14}N]_{obs} \times 2, \quad (2)$$

where subscript 'obs' represents the observed ratios or concentrations and subscript 'air' represents atmospheric values. The original gas used for the fO_2-controlled experiments have excess ^{15}N only in the form of $^{15}N^{15}N$ (mass 30), but nitrogen recovered from the run products showed excess ^{15}N both in the form of $^{15}N^{15}N$ and $^{14}N^{15}N$ (mass 29), suggesting isotopic exchange among nitrogen molecules took place during the sample synthesis. This point will be discussed later.

Pipetted air standard was repeatedly analyzed during the period of sample runs. Since the measured $^{14}N^{15}N/^{14}N^{14}N$ and $^{15}N^{15}N/^{14}N^{14}N$ ratios depend on the gas pressure, a calibration curve was obtained for $^{14}N^{15}N/^{14}N^{14}N$ against the amount of $^{14}N^{14}N$ and used for normalization.

The release profile of ^{40}Ar generally showed a large peak at ~1200°C (Appendix), suggesting that most of the dissolved Ar was released at this temperature. Sometimes ^{40}Ar release showed a minimum at around the ~600°C, suggesting that ^{40}Ar released at 400°C was an atmospheric contamination. Hence, the data of 400°C fraction (0.01–0.1% of the total extraction) were omitted from the present calculations.

On the other hand, the release profile of excess ^{15}N (L-series) often showed two peaks; a large peak at ~1200°C and a smaller peak at around ~600°C (Appendix). The former peak is considered to be the release of dissolved nitrogen as in the case for ^{40}Ar, but the latter one is most likely from organic contamination, since organic nitrogen is known to have a heavy isotopic composition (typically ~+10‰ relative to the atmospheric nitrogen). Hence, excess ^{15}N data for 400 and 600°C fractions (~1% of the total extraction) were omitted from the present calculations to avoid the effect of organic contamination.

The data were corrected for blanks and shown in Table 3a.

2.5. Solid/Melt Partition Experiment

A mixture of ~200 mg of basalt powder (Kilauea, 1921 eruption) and ~0.1 mg of ^{15}N-labeled ammonium sulfate, $(^{15}NH_4)_2SO_4$, was put in a Au_{75}-Pd_{25} capsule, sealed, and loaded in a piston-cylinder-type apparatus. At a pressure of 1.5 GPa, the sample was first heated to 1350°C for 2 h, then gradually cooled to 1270°C in 2 h 45 min, and kept at this temperature for 17 h 55 min, and quenched. The run product consisted of clinopyroxene (cpx; the average grain size was 100 μm) and glass; the volume ratio of cpx/glass was ~1. Atmospheric nitrogen and noble gases originally contained in the cavity space among basalt grains and $^{15}N^{15}N$ decomposed from ammonium sulfate were expected to be partitioned between cpx and melt. The run product was crushed to $\leq$ 50 to 60 μm, and cpx and glass (=melt) were density separated (<2.75 and >3.2 g/cm^3, respectively) using a heavy liquid (methylene iodide). Composite grains which had the density between 2.75 and 3.2 g/cm^3 were not used. The cpx/glass contamination in each phase was less than a few percent. Nitrogen and Ar were extracted from each separate by using stepwise combustion method from 600 to 1200°C with 200°C intervals and analyzed with the QMS. Extraction and analysis procedures were similar

Table 3a. Nitrogen and noble gas data for fO_2-controlled solubility experiments conducted at one atmospheric pressure.

		Synthetic condition				Concentration (mol/g)[a]			Solubility (mol/g/atm)		
Run #	Weight (mg)	Temp. (°C)	Time (h)	Starting material	log(fO_2) rel to IW	Excess $^{15}N^{15}N$ (10^{-12})	^{40}Ar (10^{-9})	^{20}Ne (10^{-12})	$K(N_2)$ (10^{-9})	K(Ar) (10^{-9})	K(Ne) (10^{-9})
L-14	55.0	1300	0.33	DB	IW + 0.9	4.67 ± 1.05	0.099 ± 0.020	5.27 ± 2.26	2.8 ± 0.6	1.9 ± 0.4	10.8 ± 4.6
L-15	93.9	1300	1	DB	IW + 0.9	7.50 ± 1.66	0.119 ± 0.025	5.42 ± 1.61	4.4 ± 1.0	2.3 ± 0.5	11.1 ± 3.3
L-16	63.8	1300	2.5	DB	IW + 0.9	8.34 ± 1.90	0.150 ± 0.031	6.11 ± 2.12	4.9 ± 1.1	2.9 ± 0.6	12.5 ± 4.3
L-17	56.4	1300	4.5	DB	IW + 0.9	7.43 ± 1.49	0.113 ± 0.024	6.02 ± 2.30	4.4 ± 0.9	2.2 ± 0.5	12.3 ± 4.7
L-18	62.6	1300	1	EB	IW + 0.9	7.91 ± 2.11	0.167 ± 0.036	7.07 ± 2.03	4.7 ± 1.2	3.2 ± 0.7	14.4 ± 4.1
L-19	41.1	1300	4.5	EB	IW + 0.9	3.15 ± 1.30	0.172 ± 0.039	6.60 ± 3.37	1.9 ± 0.8	3.3 ± 0.8	13.5 ± 6.9

[a] Typical blanks for $^{14}N^{14}N$, $^{15}N^{15}N$, ^{40}Ar and ^{20}Ne are: 8×10^{-13}, 8×10^{-17}, 8×10^{-15} and 3×10^{-15} mol for crushing, 1×10^{-12}, 1×10^{-17}, 2×10^{-13} and 3×10^{-15} for combustion at 1200°C and 3×10^{-10}, 1×10^{-16}, 2×10^{-14} and 2×10^{-15} (mol) for laser heating at 1800°C, respectively.

to those for the solubility experiments. A sector-type noble gas mass spectrometer (VG5400) was also used for the analysis of all noble gases (see Hiyagon et al., 1992, for details of the experimental procedures) and the result for Ar obtained with VG5400 was compared with that obtained with the QMS.

3. RESULTS

3.1. Gas-Melt Equilibrium

First, we examine whether the gas/melt equilibrium was attained in the present experimental conditions for the L-series samples. Figures 2a to 2c show the change in the amount of dissolved nitrogen (excess $^{15}N^{15}N$), ^{40}Ar and ^{20}Ne with time, respectively. All the samples with the synthesis times of $\geq$ 1 h (except for L-19) show essentially constant concentrations of excess $^{15}N^{15}N$, ^{40}Ar and ^{20}Ne within experimental uncertainties, suggesting equilibrium was attained within 1 h. Note that L-14 to L-17 samples were synthesized from DB (degassed basalt glass) and L-18 and L-19 were from EB (^{15}N-enriched basalt glass). In spite of a large difference in the initial $^{15}N^{15}N$ concentration between DB (~0 mol/g) and EB (19.7×10^{-12} mol/g, see Fig. 2a), the run products show almost the same $^{15}N^{15}N$ concentrations for heating times of $\geq$ 1 h. Nitrogen in L-19 shows a lower concentration, but this may be due to partial condensation of nitrogen on cold traps during gas purification. This effect was noticeable in some analyses in our earlier experiments, especially when the amount of the extracted gas was small. We tried to avoid this effect in our later experiments by controlling the liquid nitrogen level of the cold traps and it seems successful except for L-19 which is the earliest analysis among L-14 to L-19.

Dissolution equilibrium may also be supported by diffusion calculations. Diffusion coefficient of Ar in a tholeiitic basalt melt at 1350°C (6×10^{-6} cm^2/s; Lux, 1987) yields a typical diffusion length of ~1.5 mm for 1 h, which is much larger than the typical half thickness of the melt layer on the platinum mesh (~0.4 mm). Diffusion coefficient of nitrogen in synthetic melts (Na_2O-CaO-SiO_2 and R_2O-BaO-SiO_2 glasses, where R stands for alkali metals) under highly oxidizing conditions (fO_2 ~ 1 atm) was reported to be 1.8 to 5.3×10^{-6} cm^2/s at 1280 to 1400°C (Frischat et al., 1978). Assuming a similar diffusion coefficient of nitrogen for basaltic melt, we obtain a typical diffusion length of ~1 mm for 1 h, which is also larger than the half thickness of the melt layer.

For H-series samples, we only synthesized samples at 1500°C for 2 h. However, since all the samples were synthesized from fine-grained starting materials ($\leq$150 μm), we may expect equilibrium was safely attained for the H-series samples.

3.2. Solubility of Noble Gases

When Henry's law is satisfied, solubility of a gas in a melt can be expressed as a Henry's constant, i.e., a ratio of the amount of the gas dissolved in the melt to the fugacity of the gas. This is the case for noble gases (Hayatsu and Waboso, 1985; Lux, 1987; White et al., 1989; Carroll and Stolper, 1993; Miyazaki, 1996). In fact, the obtained solubilities of Ar in basaltic melt for L-series samples ($fO_2 \sim$ IW + 0.9, $P_{Ar} \sim$ 0.05 atm and $T = 1300°C$) and for H-series samples (H-10–1 to H-10–4, which were synthesized from BFa, BF7 and BF11 at $fO_2 \sim$ IW + 6.5, $P_{Ar} \sim$ 2000 atm and $T =$ 1500°C) are consistent with each other in spite of the large difference in partial pressure of Ar, as well as difference in fO_2 and temperature (2–3 $\times 10^{-9}$ mol/g/atm). They are also comparable to the results of the earlier works obtained mostly under highly oxidizing conditions (Figs. 3b and 3c) (Hayatsu and Waboso, 1985; Hiyagon and Ozima, 1986; Jambon et al., 1986; Lux 1987; Broadhurst et al., 1990; Carroll and Stolper, 1993; Marty et al., 1995; Miyazaki et al., 1995). Nearly constant solubilities of Ar and Ne independent of fO_2 are understandable since these gases are chemically inactive and dissolve physically in silicate melts. It is also apparent that solubility of Ar and Ne are not sensitive to the temperature, which corresponds to low enthalpy changes for dissolution (a few kilojoules per mole) (e.g., Hayatsu and Waboso, 1985; Lux, 1987; White et al., 1989; Carroll and Stolper, 1993).

3.3. Solubility of Nitrogen

In the case of nitrogen, Henry's law would be satisfied only when nitrogen physically dissolves in a melt as N_2. If nitrogen chemically dissolves in a melt according to a reaction N_2(gas) $\leftrightarrow$ N(melt) + N(melt), nitrogen concentration in the melt would be proportional to $(fN_2)^{1/2}$ instead of fN_2, where fN_2 is nitrogen fugacity. Here we assume Henry's law is also satisfied for nitrogen in the present experimental conditions and calculated "solubility" of nitrogen. This treatment can be justified as will be shown below. The results are listed in Tables 3a and 3b

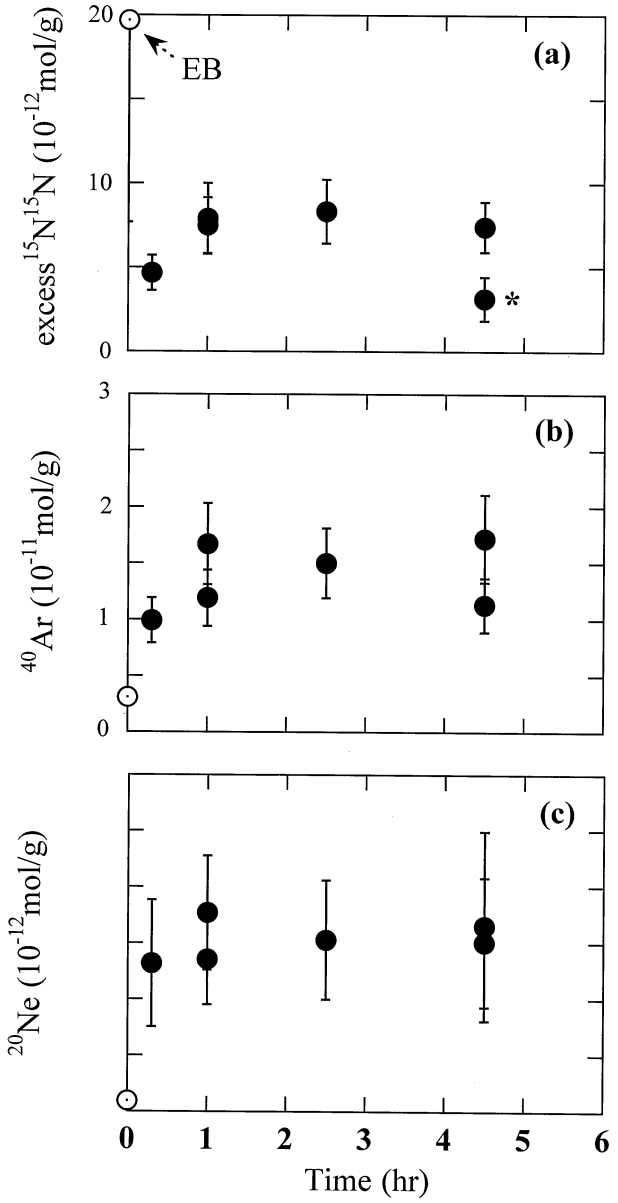

Fig. 2. Concentrations of (a) excess $^{15}N^{15}N$, (b) ^{40}Ar and (c) ^{20}Ne recovered from the samples L-14 to L-19, which were synthesized under the same condition (T = 1300°C, $fO_2 \sim$ IW + 1 and the same partial pressures of these gases) except for the heating durations (from 0.3–4.5 h). Solubility equilibrium seems to be attained within 1 h for all the gases. Note that two samples (L-18 and L-19) were synthesized from EB (^{15}N-enriched basalt glass; shown in [a]), while the others from DB (degassed basalt glass); both groups, however, show similar results in spite of their different initial ^{15}N concentrations. (*Nitrogen might be partially condensed on cold traps. See text.)

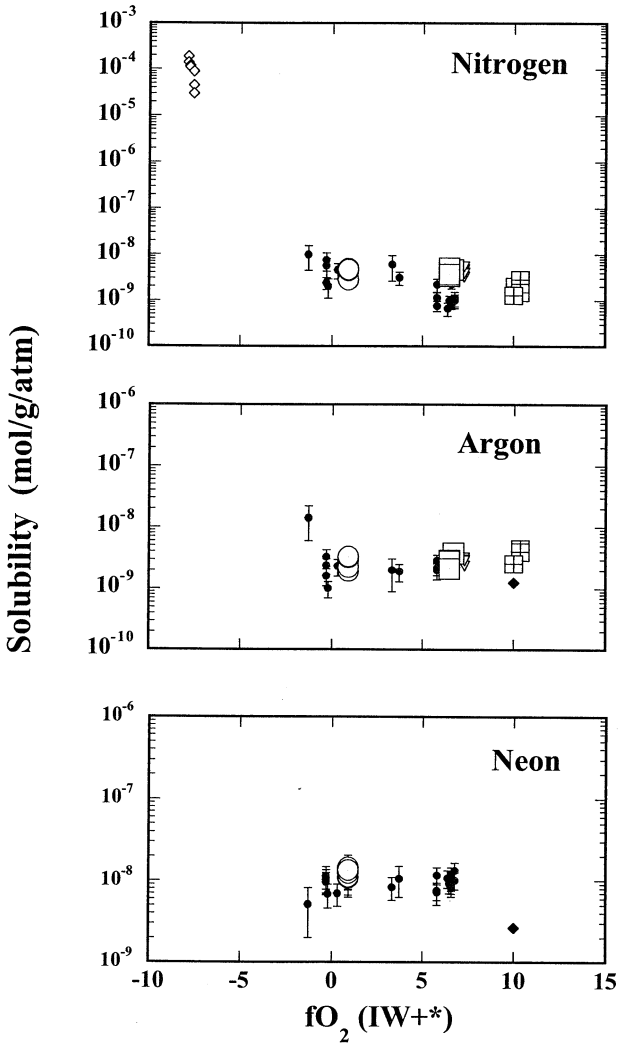

Fig. 3. Solubilities of (a) nitrogen, (b) Ar and (c) Ne in basalt melt obtained from L-series (fO_2 = IW + 1.4 and T = 1300°C) and H-series (fO_2 = IW + 6 and T = 1500°C) samples. Also shown are the results of previous works and our earlier data (Miyazaki, 1996). Constant solubilities of nitrogen from $fO_2 \sim$ IW to IW + 10 are compatible with physical dissolution as N_2 molecules, as was reported at highly oxidizing conditions (Miyazaki et al., 1995). In contrast, very high solubilities reported at $fO_2 \sim$ IW − 8 (Fogel, 1994) may be caused by chemical dissolution of nitrogen in the melt. The broken line shows the expected fO_2-dependence (slope = –3/4) assuming a chemical reaction (see text).

and plotted in Figure 3a as a function of oxygen fugacity. For comparison, also shown are the results of previous works and our earlier data (Miyazaki et al., 1995; Miyazaki, 1996).

The present results for nitrogen in basaltic melt obtained at fO_2 = IW + 0.9 (L-series samples) and at fO_2 = IW + 6.5 (H-series samples) are consistent with our earlier results obtained at highly oxidizing conditions ($fO_2 \sim$ IW + 10; Miyazaki et al., 1995) and with the results by Marty et al. (1995), but much lower than the results by Fogel (1994) obtained at highly reducing conditions ($fO_2 \sim$ IW − 8). Nitrogen solubility does not show significant changes between 1300°C at low pressures (L-series samples) and 1500°C at high pressures (H-series samples). This suggests that (1) the enthalpy change for dissolution of nitrogen is also low, probably of the order of a few kilojoules per mole, and that (2) Henry's law is satisfied for fN_2 of up to ~250 atm (2.5×10^7 Pa), which is consistent with Kesson and Holloway (1974). Our earlier data obtained at 1300°C and $fO_2 \geq$ IW − 1 (Miyazaki, 1996) also show comparable nitrogen solubility, though they have larger errors.

Table 3b. Nitrogen and noble gas data for solubility experiments conducted at high pressures.

		Synthetic condition				Concentration (mol/g)		Solubility (mol/g/atm)	
Run #	Weight (mg)	Temp. (°C)	Time (h)	Starting material	log(fO_2) rel to IW	$^{14}N^{14}N$ (10^{-6})	^{40}Ar (10^{-6})	$K(N_2)$ (10^{-9})	K(Ar) (10^{-9})
H-9	7.75	1500	2	AND	IW + 6.7	1.143 ± 0.284	10.21 ± 2.10	4.63 ± 1.15	3.82 ± 0.79
H-10-1	13.82	1500	2	BFa	IW + 6.5	0.871 ± 0.180	7.10 ± 1.44	4.12 ± 0.85	2.92 ± 0.59
H-10-2	71.60	1500	2	BF7	IW + 6.5	1.080 ± 0.224	5.52 ± 1.12	5.10 ± 1.06	2.27 ± 0.46
H-10-3	8.34	1500	2	BF11	IW + 6.5	0.710 ± 0.151	6.80 ± 1.39	3.36 ± 0.71	2.80 ± 0.57
H-10-4	18.61	1500	2	BFI11	IW + 6.5	0.776 ± 0.162	5.21 ± 1.06	3.67 ± 0.77	2.15 ± 0.44
H-10-5	30.62	1500	2	DA	IW + 6.5	0.091 ± 0.019	0.92 ± 0.19	0.43 ± 0.09	0.38 ± 0.08

All these observations support physical dissolution of nitrogen in silicate melts for fO_2 from ~IW + 10 down to ~IW.

The obtained solubilities (Henry's constants) of Ar (2–3 × 10^{-9} mol/g/atm) and Ne (11–14 × 10^{-9} mol/g/atm) are consistent with the results of previous works: K(Ar) = 1.3 to 4.9 × 10^{-9} mol/g/atm and K(Ne) = 3 to 16 × 10^{-9} mol/g/atm (Hayatsu and Waboso, 1985; Hiyagon and Ozima, 1986; Jambon et al., 1986; Lux, 1987; Broadhurst et al., 1992; Carroll and Stolper, 1993). The obtained solubilities of nitrogen show larger variations than those for Ar and Ne, but the overall results consistently suggest that solubility of nitrogen in silicate melts is comparable to that of Ar. This is also consistent with the results by Cartigny et al. (2001), who estimated the ratio of Ar solubility/N_2 solubility to be ~1.2 based on the C-N-Ar isotope systematics in MORB glasses.

The present solubility trend (Ne > Ar ~ N_2) is roughly anticorrelated with molecular diameters of the gases (234, 286 and 316 nm for Ne, Ar and N_2, respectively, estimated from the gas viscosities; Moore, 1962), which is consistent with the trend reported for noble gas solubilities (Blander et al., 1958; Kirsten, 1968; Lux, 1987; Broadhurst et al., 1992).

3.4. Dependence on Melt Compositions

Solubility of nitrogen seems to depend on melt compositions, which may be explained by the change in their polymerization as was suggested for noble gases (White et al., 1989; Montana et al., 1993; Shibata et al., 1996). The highest nitrogen solubility was obtained for andesite melt, which has the highest concentration of network forming cations, Si^{4+} and Al^{3+} (57.2 wt.% SiO_2 and 17.5 wt.% Al_2O_3; Table 2), and hence, is more polymerized than basalt melt (e.g., 47.5 wt.% SiO_2 and 13.5 wt.% Al_2O_3 for BFI). In contrast, the lowest nitrogen solubility was obtained for $Di_{64}An_{36}$ melt, which is less polymerized than basalt melt due to its higher concentrations of network modifier cations such as Ca^{2+} and Mg^{2+} (23.8 wt.% CaO and 11.9 wt.% MgO) (Mysen, 1986).

3.5. Isotopic Compositions of Nitrogen Recovered From L-Series Samples

The changes in the isotopic composition of nitrogen during the analyses with the QMS are plotted on the (mass 30/mass 28) vs. (mass 29/mass 28) diagrams; Figures 4a and 4b show data for the gases recovered from L-4 (earlier data) and L-16. Also shown for references are the isotopic compositions of atmospheric nitrogen (A), $^{15}N^{15}N$-labeled gas used for the synthesis (G) and its isotopically equilibrated composition (E). When the gas enriched in $^{15}N^{15}N$, such as $^{15}N^{15}N$-labeled gas, are loaded to QMS, the hot tungsten filament would promote equilibration of nitrogen molecules through the reaction,

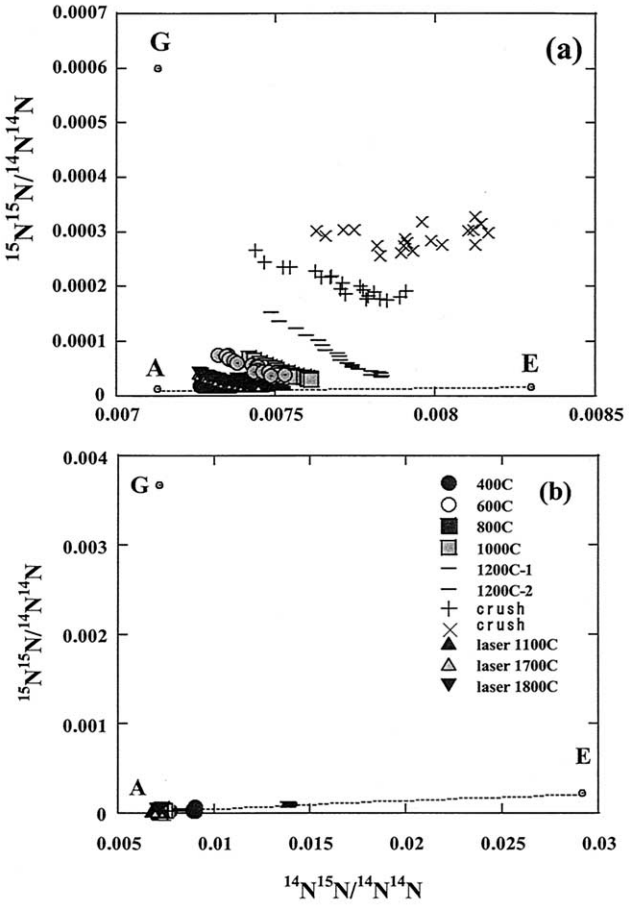

Fig. 4. Changes in the isotopic composition of nitrogen ($^{15}N^{15}N/^{14}N^{14}N$ vs. $^{14}N^{15}N/^{14}N^{14}N$) during the QMS analyses for the gases extracted from (a) L-4 (fO_2 = IW + 6) and (b) L-16 (fO_2 = IW + 0.9). The data are not hot blank-corrected. Also shown for references are the compositions of the air (A), the $^{15}N^{15}N$-labeled gas (G) and its isotopically equilibrated composition (E). The isotopic exchange among nitrogen molecules would shift the data from upper left to lower right in the diagram with a slope of –1/2 (parallel to [G]-[E] line). The effect clearly be seen for the gas extracted at 1200°C from L-4 sample (a).

Table 4. Nitrogen and noble gas data for the cpx/melt partition experiment.

				Concentration (mol/g)					
Sample #	Phase	Weight (mg)	Temp. (°C)	Excess ^{15}N (10^{-9})	^{4}He (10^{-12})	^{20}Ne (10^{-12})	^{40}Ar (10^{-9})	^{84}Kr (10^{-12})	^{132}Xe (10^{-12})
QMS data									
KB01-GL	glass	1.26	600	0.1 ± 0.1			0.4 ± 0.1		
			800	30.4 ± 6.1			9.2 ± 1.8		
			1000	1440 ± 288			254 ± 51		
			1200	41.2 ± 8.2			8.2 ± 1.6		
			1200	0.0 ± 0.0			0.0 ± 0.0		
			Total	**1510 ± 290**			**272 ± 51**		
KB01-CPX	cpx	2.04	600	0.4 ± 0.1			0.2 ± 0.0		
			800	7.2 ± 1.4			1.8 ± 0.4		
			1000	79.7 ± 15.9			26.0 ± 5.2		
			1200	4.6 ± 0.9			1.6 ± 0.3		
			1200	0.0 ± 0.0			0.0 ± 0.0		
			Total	**92 ± 16**			**29.6 ± 5.2**		
VG5400 data									
KB01-GL	glass	1.19	1700		**260 ± 28**	**450 ± 50**	**204 ± 20**	**18.0 ± 3.0**	**0.60 ± 0.10**
KB01-CPX	cpx	1.18	600		5 ± 10	54.9 ± 6.6	0.17 ± 0.02	0.01 ± 0.00	0.000 ± 0.000
			1700		14 ± 10	1.7 ± 0.4	24.4 ± 2.5	1.84 ± 0.28	0.081 ± 0.012
			Total		**19 ± 14**	**57 ± 6**	**24.5 ± 2.5**	**1.85 ± 0.28**	**0.081 ± 0.012**

	Partition coefficient (cpx/melt)					
	N	He	Ne	Ar	Kr	Xe
QMS data	0.06 ± 0.02			0.11 ± 0.03		
VG5400 data		0.07 ± 0.05	0.13 ± 0.02	0.12 ± 0.02	0.10 ± 0.02	0.14 ± 0.03

$^{15}N^{15}N + {}^{14}N^{14}N \leftrightarrow 2{}^{14}N^{15}N$ during the analysis (Miyazaki et al., 1995). Since the amount of $^{14}N^{14}N$ is almost constant due to its high abundance, this reaction would move the data points from upper left to lower right in the diagram with a slope of −1/2, parallel to (G)-(E) line. This effect can clearly be seen for the gas extracted at 1200°C from L-4 sample (Fig. 4a) that was synthesized under relatively oxidizing condition (fO_2 = IW + 6). Note that the amounts of nitrogen extracted from L-4 sample by crushing were negligibly small (<1% of total extraction) and their isotopic composition showed the characteristics of $^{15}N^{15}N$-enriched component but was possibly affected by the interferences of CO. In contrast, all the data points for L-16, synthesized at fO_2 = IW + 0.9, make clusters along the A-E line (Fig. 4b), suggesting isotopic exchange has been completed before the analysis. All other samples synthesized at fO_2 = IW + 0.9 and ≥ 1 h also show equilibrated isotopic compositions of nitrogen. A question is when and where isotopic exchange took place. As will be discussed later, such isotopic exchange is not directly related to dissociation of nitrogen molecules in silicate melts (i.e., chemical dissolution of nitrogen) and is not in contradiction to physical dissolution of nitrogen.

3.6. Solid/Melt Partition Coefficients

The obtained nitrogen and noble gas concentrations in clinopyroxene (cpx) and basaltic glass (melt) fractions and the calculated cpx/melt partition coefficients are summarized in Table 4.

The results for Ar, measured using both QMS and VG5400 systems, are consistent with each other within experimental uncertainties. The obtained cpx/basaltic melt partition coefficients for noble gases are 0.10 to 0.14, which are in the same order as the olivine/basaltic melt partition coefficients obtained by Hiyagon and Ozima (1986). (Data for He are omitted from the present discussion because of a large hot blank relative to the amount of He in sample.) While the obtained cpx/melt partition coefficient for nitrogen is 0.06, that is, slightly lower than those for Ar and other noble gases. This suggests that nitrogen is slightly more incompatible than noble gases in the cpx-basaltic melt system. It is interesting to note that nitrogen, which must be chemically more active than noble gases, shows higher incompatibility than noble gases.

Nitrogen extracted from both cpx and glass was isotopically almost equilibrated, that is, ~97% of the added ^{15}N was observed in the form of $^{14}N^{15}N$. This suggests that isotopic exchange between the chemically added ^{15}N and normal N_2 in air contained in cavity spaces among basalt grains in the sample capsule must have taken place during the sample synthesis.

4. DISCUSSION

4.1. Nitrogen Dissolution Mechanism

Nitrogen physically dissolves in basalt melt under highly oxidizing conditions (Miyazaki et al., 1995), whereas nitrogen chemically dissolves in silicate melts as nitrides (Si-N) or cyanides (C-N) under highly reducing conditions (e.g., Tsukihashi et al., 1985; Ito and Fruehan, 1988; Martinez and Sano, 1990). In this section, we discuss dissolution mechanisms of nitrogen in the present experimental conditions (fO_2 ≥ IW).

Since no graphite was used in our solubility experiment, cyanide fugacity in the system was calculated to be very low ($fCN^- < 10^{-44}$ atm), so that nitrogen dissolution as cyanide ion (CN^-) can be ignored. Ryall and Muan (1969) reported that silicon oxynitride is stable in the system Si-O-N when $P(N_2)/P(O_2) > 10^{15}$ at 1400 to 1500°C. In our L-series solubility experiments, where $P(N_2)$ was kept at ~0.5 atm, silicon oxynitride is stable at $P(O_2) < 10^{-16}$ atm or $fO_2 <$ IW − 7 at 1300°C. Therefore, formation of oxynitrides can be ignored in the present L-series samples.

More recently, Ito and Fruehan (1988) proposed a reaction formula on nitrification dissolution in a $CaO\text{-}SiO_2\text{-}Al_2O_3$ melt as

$$1/2(N_2) + 3/4(SiO_2) = (Si_{0.75}N) + 3/4(O_2) \quad (3)$$

based on the observed $P(N_2)$ and fO_2 dependence of nitrogen solubility, i.e., the amount of nitrogen dissolved as nitride in the silicate melt is (1) proportional to $(fO_2)^{-3/4}$ and (2) proportional to $P(N_2)^{1/2}$. Moreover, nitrification process was reported to be an endothermic process, that is, (3) the amount of nitrogen increases with increasing temperature, and the enthalpy change on solution was given as 420 kJ/mol for a $CaO\text{-}Al_2O_3$ melt (Shimoo et al., 1972).

On the other hand, the present results show that (1) the enthalpy change for dissolution of nitrogen is low, probably of the order of a few kilojoules per mole, and that (2) Henry's law is satisfied for fN_2 of up to ~250 atm (2.5×10^7 Pa). These characteristics are compatible with physical dissolution in melts as N_2 molecules. Moreover, almost constant N_2/Ar ratios (1–2) in various silicate melts suggest that nitrogen and Ar probably occupy similar sites in silicate melts. All these observations suggest physical dissolution of nitrogen, while the isotopic data (Fig. 4) seem contradictory to this conclusion. However, we will show below that the isotopic data also are not inconsistent with the physical dissolution.

As is shown in the previous section, the isotopic composition of nitrogen recovered from the L-16 samples (synthesized at fO_2 = IW + 0.9) is completely equilibrated. If isotopic exchange is associated with dissociation of N_2 molecules in the melt (i.e., chemical dissolution), nitrogen solubility must change significantly, but this is not the case. The question is where the isotopic exchange occurred.

It is not likely that the isotopic exchange occurred in the ambient gas phase during the sample synthesis, because the energy for dissociation of N_2 molecules (900 kJ/mol) is too high to take place at 1300°C.

The platinum mesh involved in the melt, which was alloyed with iron in the basalt melt (analyzed with EPMA), is a candidate of the efficient catalyst for dissociation of N_2 molecules. However, since $^{15}N^{15}N$-labeled gas was continuously supplied from the melt surface, the proportion of isotopically equilibrated nitrogen in the melt could be at most ~50% in the steady state. This is not the case for L-series samples, for which almost complete isotopic equilibration is observed. Therefore, platinum mesh is not likely to be the cause for the isotopic exchange of nitrogen.

We speculate that the isotopic exchange might take place on the surface of the melt. In this model, nitrogen molecules adsorbed on the surface of the melt becomes dissociated into nitrogen atoms. However, when the dissociated nitrogen atoms are incorporated into melt or released to the gas phase, they are recombined to form N_2 molecules without any preference for isotopes. This model is compatible with the results obtained by Ono et al. (1997), who found that the rate of N_2 isotopic exchange in the reaction, $^{15}N^{15}N + {}^{14}N^{14}N \leftrightarrow 2 \times {}^{14}N^{15}N$, was constant at $fO_2 < 10^{-13}$ atm (<IW − 5) when N_2 coexisted with a $CaO\text{-}Al_2O_3$ melt at 1600°C but that the amount of nitrogen dissolved in this melt increased with decreasing fO_2. This suggests that the isotopic exchange is not related to nitrogen dissolution in the melt. Ono et al. (1997) also reported that the rate of isotopic exchange decreased with increasing fO_2 for $fO_2 > 10^{-12}$ atm (i.e., >IW − 4). This is consistent with the observation that the recovered nitrogen was less equilibrated for the samples equilibrated at higher fO_2 (Miyazaki et al., 1995; Miyazaki, 1996). A possible interpretation for this is, under the oxidizing condition, the adsorption (and dissociation) sites of nitrogen on the melt surface are more easily occupied by oxygen, which would prevent dissociation (and hence isotopic exchange) of nitrogen. Note that the isotopically equilibrated nitrogen produced in this process cannot be detected in the gas phase in the present experimental settings; the reported isotopic exchange rate ($<10^{-7}$ mol N_2/s/cm^2 of the melt surface/atm of N_2 gas), $P(N_2)$ = 0.5 atm, the surface area of the melt ~ 2 cm^2, and the gas flow rate of 8 to 10 cm^3/s would give only $< 5 \times 10^{-5}$ for the fraction of the isotopically equilibrated nitrogen.

In summary, we conclude that the observed isotopic exchange most probably occurred on the melt surface and might not have affected the mechanism of nitrogen dissolution in the present experimental conditions for L-series samples; in other words, nitrogen physically dissolved in silicate melts at $fO_2 >$ IW.

4.2. Effect of fO_2 on Nitrogen Solubility Under $fO_2 <$ IW

Very high solubilities obtained by Fogel (1994) are most likely due to chemical dissolution of nitrogen in the melt. Assuming the chemical dissolution process given by Eqn. 3, the amount of chemically dissolved nitrogen rapidly decreases with increasing fO_2 with a slope of −3/4 in the log(solubility)-log(fO_2) diagram (Fig. 3a). If we extrapolate Fogel's data toward a higher fO_2 along this trend, chemically dissolved nitrogen would become negligibly small at $fO_2 \geq$ IW − 2. This view is supported by a recent preliminary work by Humbert (1998), in which they conducted solubility experiments for nitrogen in iron-free silicate.

4.3. $N_2/^{36}Ar$-Fractionation Between the Mantle and the Atmosphere

Based on the present results, we will discuss below the origin and evolution of nitrogen and Ar in the Earth.

The present results show that, at $fO_2 \geq$ IW, (1) solubility of nitrogen in silicate melts is comparable to that of Ar and (2) cpx/melt partition coefficient of nitrogen is comparable to or slightly lower than that of Ar. The experimental conditions cover possible oxidation states of the mantle from the early Earth to the present. An important inference of this result is that large nitrogen/Ar fractionation between the atmosphere (N_2/

$^{36}Ar \sim 10^4$) and the mantle ($>10^6$) cannot be produced through magmatic processes even in the early history of the Earth, where relatively low oxygen fugacity (~IW) was expected.

Tolstikhin and Marty (1998) proposed an evolution model of noble gases (He, Ne and Ar) and nitrogen to explain the isotopic compositions of these gases in the atmosphere and the mantle. They argued that nitrogen solubility in the magma ocean might be much higher than Ar solubility under a low fO_2 condition (~IW) in the early Earth and that nitrogen would have been preferentially partitioned into the magma ocean, which resulted in the higher $N_2/^{36}Ar$ ratio in the present mantle. However, the present results clearly show that this is not the case.

4.4. Equilibrium Distribution Among Different Reservoirs

First we consider the case for equilibrium distribution of nitrogen and Ar among the atmosphere, magma ocean (Abe and Matsui, 1985) and the core. The amount of nitrogen and $N_2/^{36}Ar$ ratio in the present atmosphere are $\sim 4 \times 10^{21}$ g and $\sim 2 \times 10^4$, respectively. The amount of nitrogen and $N_2/^{36}Ar$ ratio for the molten mantle, which we assume here to be equilibrated with the present atmosphere, are calculated to be $\sim 2 \times 10^{20}$ g and $\sim 10^4$, respectively, using the solubilities of nitrogen and Ar in silicate melts obtained in the present study.

The magma ocean eventually became solidified, and nitrogen and noble gases once having dissolved in it might be expelled out from the solidifying mantle to the atmosphere because of their low crystal/silicate melt partition coefficients (~0.1). Further magmatic activities (production of magma in the mantle and its transportation to the Earth's surface) will transport nitrogen and noble gases efficiently from the mantle to the atmosphere. However, these magmatic processes would not produce large nitrogen/Ar fractionation in the mantle, as was discussed earlier.

The partition coefficient of nitrogen between silicate melt and molten iron at fO_2 = IW can be calculated using solubility of nitrogen in silicate melt and that in molten iron (e.g., Kasamatsu and Matoba, 1959; Gomersall et al., 1968). The solubility in molten iron is reported to be 0.45 wt.% or 1.6×10^{-4} mol/g at 1600°C at 1 atm of N_2; it should be noted that the amount of dissolved nitrogen changes proportional to $P(N_2)^{1/2}$, because nitrogen molecules become dissociated in molten iron. Since nitrogen dissolves in silicate melt according to Henry's law ($\propto P[N_2]$) at fO_2 = IW, the metal/silicate melt partition coefficient of nitrogen changes with $P(N_2)^{-1/2}$. Assuming $P(N_2) = 1$ atm in the atmosphere, the nitrogen concentrations in silicate melt and molten iron equilibrated with the atmosphere are calculated to be ~0.05 and ~500 ppm, respectively. Hence we obtain the metal/silicate melt partition coefficient for nitrogen to be $\sim 10^4$ at $P(N_2) = 1$ atm. This gives the amount of nitrogen in the core to be $\sim 1 \times 10^{24}$ g, suggesting that the major reservoir of nitrogen is the core. Matsuda et al. (1993) reported iron melt/silicate melt partition coefficients for noble gases at high pressures and found that they rapidly decrease with increasing pressures (down to the order of $\sim 10^{-4}$ at 10 GPa). This suggests that the amount of noble gases (Ar) partitioned into the core is negligibly small compared with that of the atmosphere. The major reservoir of Ar (noble gases) is, therefore, the atmosphere. The $N_2/^{36}Ar$ ratio in the core is expected to be very high (e.g., $>10^9$).

These equilibrium (magmatic) distributions of nitrogen and Ar would produce comparable nitrogen/Ar ratio both in the mantle and in the atmosphere. If nitrogen in the atmosphere was preferentially transferred to the mantle or a small fraction of the core component was added to the mantle, the $N_2/^{36}Ar$ ratio in the mantle would increase. To understand the $N_2/^{36}Ar$ fractionation between the mantle and the atmosphere, we will discuss below these two possible processes,: nitrogen subduction and "inefficient core formation" model. Between them, we consider an "insufficient core formation" model to be more likely.

4.5. Nitrogen Subduction

Nitrogen is contained both physically and chemically in sediments and (altered) crust, while Ar is trapped only physically. Hence, nitrogen in the surface reservoirs would be preferentially recycled to the mantle through subduction compared with the case for Ar. This would increase the $N_2/^{36}Ar$ ratio in the mantle throughout the Earth's history, thus may be a possible process to fractionate the $N_2/^{36}Ar$ ratio between the mantle and the atmosphere. This process, however, seems unlikely in view of nitrogen isotopes.

Most of the mantle-derived materials show isotopic composition of ($\delta^{15}N$) a few to 10‰ lower than that in the atmosphere (defined as $\delta^{15}N = 0$‰). In diamonds, $\delta^{15}N$ values mostly range from −8 to −4‰ and such samples generally show characteristic carbon isotopic compositions in the mantle ($\delta^{13}C \sim -5$‰ on the PDB scale) (Javoy et al., 1984; Boyd et al., 1987, 1992; Boyd and Pillinger, 1994; Cartigny et al., 1997, 1998). In MORB glasses, the average $\delta^{15}N$ values are reported to be −4.5 to −1.7‰ (Javoy and Pineau, 1991; Marty et al., 1996; Marty and Zimmermann, 1999; Nishio et al., 1999). Fluid inclusions in the mantle xenolith also showed $\delta^{15}N \sim -5$‰ (Nadeau et al., 1990). All these observations suggest that nitrogen in the mantle is isotopically lighter than that in the atmosphere by a few to 10‰.

On the other hand, nitrogen contained in sediments or metamorphic rocks in the subduction zone, which is chemically trapped in the form of organic nitrogen or ammonium ions, tend to have heavy isotopic compositions ($\delta^{15}N \sim +1$ to +10‰; Peters et al., 1978; Haendel et al., 1986; Bebout and Fogel, 1992; Boyd et al., 1993; Bebout, 1997). Furthermore, $\delta^{15}N$ in meta-sedimentary rocks were reported to increase with increasing metamorphic grade, (Haendel et al., 1986; Bebout and Fogel, 1992; Bebout, 1997). Hence, subduction would supply isotopically heavy nitrogen ($\delta^{15}N \sim +10$‰.) to the mantle. If such a return flux of nitrogen is responsible for the two orders of magnitude enrichment of the $N_2/^{36}Ar$ ratio in the mantle compared with that of the atmosphere, nitrogen in the mantle must have become isotopically heavy. Even if the primitive mantle had the $\delta^{15}N$ value of as low as −25‰, the lowest mantle value ever found in mantle derived materials (Fuxian diamond, China; Cartigny et al., 1997), addition of such a large amount of ^{15}N-enriched surface nitrogen would increase the isotopic composition quite similar to the surface value ($\delta^{15}N \sim +10$‰).

Recently, ^{15}N-depleted nitrogen is found in kerogens in early

Archean cherts (Beaumont and Robert, 1999) and isotopically light nitrogen could recycle into the ancient mantle. However, this component would be negligible, since it is considered to be produced by chemoautolithotrophic bacteria around hydrothermal vent (Pinti and Hashizume, 2001) and the output (or the rate of deposition) might be much smaller than that at present.

4.6. Inefficient Core Formation

"Inefficient core formation" model is similar to that proposed by Jones and Drake (1986). Highly siderophile elements, such as Os, Re, Ir, Pt, etc., are known to be enriched in the mantle than would be expected assuming equilibrium distribution between the core (metal) and the magma ocean (silicate). The abundance pattern of these elements in the upper mantle shows nearly uniform depletion relative to the solar abundance and Si (e.g., Jagoutz et al., 1979; Sun, 1982; Chou et al., 1983) in spite of their difference in siderophile nature. Here we assume that a small fraction of metallic iron failed to segregate into the core and it eventually became oxidized and mixed with the silicate mantle. About 0.5 to 1 wt.% of metallic iron can explain the abundances of highly siderophile elements in the present mantle (0.003–0.005 relative to Si and CI; Kargel and Lewis, 1993). Metallic iron, equilibrated with the magma ocean, would contain 500 ppm of nitrogen but negligible amount of noble gases (Matsuda et al., 1993). Since metallic iron/silicate melt partition coefficient of nitrogen is $\sim 10^4$, the "inefficient core formation" model can produce large $N_2/^{36}Ar$ fractionation. Addition of 0.5 to 1 wt.% of metallic iron containing 500 ppm nitrogen would result in 2.5 to 5 ppm nitrogen in the present mantle. This is higher than the present estimates in the mantle of $N_2 \sim 1.6$ ppm based on MORB glass data (Norris and Schaeffer, 1982) and ~0.1 to 0.2 ppm based on N_2 flux from the mantle (Zhang and Zindler, 1993; Marty and Zimmerman, 1999) but may be reasonable if we consider a later degassing of nitrogen from the mantle through solidification of the magma ocean and through continuing magmatic activities.

Slightly lighter isotopic composition of nitrogen in the mantle ($\delta^{15}N$ of a few to 10‰ lower) compared with that in the atmosphere may be explained by the presence of slightly ^{14}N-rich primitive nitrogen in earlier stages of the Earth's accretion, that is, addition of meteoritic volatiles which is an assumption similar to that adopted by Javoy (1998) and Tolstikhin and Marty (1998). Alternatively, a small effect of hydrodynamic escape may also explain the isotopic difference in the mantle and the atmosphere.

5. SUMMARY

Solubility experiments for nitrogen and noble gases (Ar and Ne) in silicate melts (mostly of basaltic composition) were performed using two experimental configurations: one (L-series) conducted at one atmospheric pressure, $T = 1300$°C and $fO_2 = IW + 0.9$, and the other (H-series) at high pressures ($P_{total} \sim 2 \times 10^8$ Pa and fN_2 up to $\sim 2.5 \times 10^7$ Pa), $T = 1500$°C and $fO_2 \sim IW + 6$. For the L-series experiments, isotopically labeled-nitrogen was used to distinguish dissolved nitrogen from contaminating atmospheric or organic nitrogen and to examine dissolution mechanisms of nitrogen in silicate melts. A preliminary experiment was also performed for partitioning of nitrogen and noble gases between clinopyroxene (cpx) and basaltic melt using a piston cylinder-type apparatus at 1.5 GPa and at 1270 to 1350°C. Based on the present results, combined with our earlier results (Miyazaki et al., 1995; Miyazaki, 1996), we discussed the origin and evolution of nitrogen and Ar in the mantle and the atmosphere of the Earth. The followings are the summary of the present study.

1. For nitrogen dissolution in silicate melts, Henry's law is satisfied for fN_2 of up to ~250 atm (2.5×10^7 Pa).
2. Solubility (Henry's constant) of nitrogen in basalt melt is independent of fO_2 from ~IW + 10 down to ~IW.
3. Solubility of nitrogen shows only a weak temperature dependence, similar to the case for noble gases, which corresponds to a low enthalpy change (probably a few kilojoules per mole).
4. The results (1) to (3) support physical dissolution of nitrogen as N_2 molecules in silicate melts for fO_2 from ~IW + 10 down to ~IW.
5. The obtained solubility of nitrogen is 3 to 5×10^{-9} mol/g/atm. This is comparable to that of Ar ($2–4 \times 10^{-9}$ mol/g/atm), and much lower than that of Ne ($11–14 \times 10^{-9}$ mol/g/atm).
6. Isotopic compositions of nitrogen recovered from the samples synthesized at $fO_2 = IW + 0.9$ (L-series) were almost equilibrated. Isotopic exchange among nitrogen molecules might take place on the surface of the silicate melt. They might become recombined to molecules when nitrogen dissolved in the melt.
7. The obtained cpx/melt partition coefficient of nitrogen is ~0.06, which is slightly lower than those of noble gases (~0.1 for Ne to Xe).
8. The present results suggest that nitrogen behaves as incompatible as or even slightly more incompatible than Ar in the silicate mantle throughout the history of the Earth (at $fO_2 \geq$ IW). Therefore, magmatic processes are not responsible for the two orders of magnitude difference in the $N_2/^{36}Ar$ ratio between the present atmosphere ($\sim 10^4$) and the mantle ($\sim 10^6$).
9. We examined two possibilities to explain the $N_2/^{36}Ar$ fractionation between the mantle and the atmosphere, such as preferential recycling of nitrogen into the mantle through subduction and an "inefficient core formation" model. Between them, we suggested the "inefficient core formation" is more likely. In this model, it is assumed that a small fraction of the metallic iron failed to segregate into the core, which eventually became oxidized and mixed with the mantle. Since nitrogen has a siderophile nature, such a process would significantly enhance the $N_2/^{36}Ar$ ratio in the mantle.

Acknowledgments—We thank Dr. M. Nakamura for help in synthesizing samples with a gas-medium high pressure apparatus at Tokyo Institute of Technology, Dr. Y. Koizumi for help in Mössbauer spectroscopy at the Radioisotope Center, University of Tokyo, Dr. Y. Minai for providing the analysis program of the Mössbauer spectra, O. Tachikawa for help in EPMA analysis. We also thank Dr. K. Hashizume and Dr. K. Kiyota for their advice and suggestions on nitrogen and noble gas analyses using QMS, and Dr. T. Shibata for valuable suggestions on solubility experiments. Thanks are also expressed to Prof. M. Ozima, Prof. I. Kaneoka, Dr. K. Kuramoto, Dr. G. Hashimoto and Dr. Y. N. Miura for helpful discussions and encouragements. The manuscript was greatly improved by helpful comments and suggestions

of Prof. J. Matsuda, Prof. S. V. S. Murty, Dr. E. F. Baxter and Dr. D. L. Pinti. This work was financially supported in part by a Grant-in-Aid for scientific Research from the Ministry of Education, Science and Culture, Japan (no. 07454138 for H. H.).

Associate editor: J. Matsuda

REFERENCES

Abe Y. and Matsui T. (1985) The formation of an impact-generated H_2O atmosphere and its implications for the early thermal history of the Earth. *J. Geophys. Res.* **90,** C545–C559.

Arculus R. J. (1985) Oxidation status of the mantle: Past and present. *Ann. Rev. Earth Planet. Sci.* **13,** 75–95.

Bebout G. E. (1997) Nitrogen isotope tracers of high-temperature fluid-rock interactions: Case study of the Catalina Schist, California. *Earth Planet. Sci. Lett.* **151,** 77–90.

Bebout G. E. and Fogel M. (1992) Nitrogen-isotope compositions of metasedimentary rocks in the Catalina Schist, California: Implications for metamorphic devolatilization history. *Geochim. Cosmochim. Acta* **56,** 2839–2849.

Beaumont V. and Robert F. (1999) Nitrogen isotopic ratios of kerogens in Precambrian cherts: a record of the evolution of atmospheric chemistry? *Precam. Res.* **96,** 63–82.

Blander M., Grimes W. R., Smith N. V., and Watson G. M. (1958) Solubility of molten fluorides. II. In the LiF-Na-K-KF eutectic mixture. *J. Phys. Chem.* **63,** 1164–1167.

Boyd S. R. and Pillinger C. T. (1994) A preliminary study of $^{15}N/^{14}N$ in octahedral growth from diamonds. *Chem. Geol.* **116,** 43–59.

Boyd S. R., Mattey D. P., Pillinger C. T., Milledge H. J., Mendelssoon M., and Seal M. (1987) Multiple growth events during diamond genesis: An integrated study of carbon and nitrogen aggregation state in coated stones. *Earth Planet. Sci. Lett.* **86,** 341–353.

Boyd S. R., Pillinger C. T., Milledge H. J., Mendelssoon M., and Seal M. (1992) C and N isotopic composition and the infrared absorption spectra of coated diamonds: evidence for the regional uniformity of CO_2-H_2O rich fluids in lithospheric mantle. *Earth Planet. Sci. Lett.* **109,** 633–644.

Boyd S. R., Hall A., and Pillinger C. T. (1993) The measurement of $\delta^{15}N$ in crustal rocks by static vacuum mass spectrometry: Application to the origin of the ammonium in the Cornubian batholith, southwest England. *Geochim. Cosmochim. Acta* **57,** 1339–1347.

Broadhurst C. L., Drake M. J., Hagee B. E., and Bernatowicz T. J. (1990) Solubility and partitioning of Ar in anorthite, diopside, forsterite, spinel, and basaltic liquids. *Geochim. Cosmochim. Acta* **54,** 299–309.

Broadhurst C. L., Drake M. J., Hagee B. E., and Bernatowicz T. J. (1992) Solubility and partitioning of Ne, Ar, Kr, and Xe in minerals and synthetic basaltic melts. *Geochim. Cosmochim. Acta* **56,** 709–723.

Brooker A. R., Wartho J.-A., Carroll M. R., Kelly S. P., and Draper D. S. (1998) Preliminary UVLAMP determinations of argon partition coefficients for olivine and clinopyroxene grown from silicate melts. *Chem. Geol.* **147,** 185–200.

Canil D., O'Neill H. S., Pearson D. G., Rudnick R. L., McDonough W. F., and Carswell D. A. (1994) Ferric iron in peridotites and mantle oxidation states. *Earth Planet. Sci. Lett.* **123,** 205–220.

Carroll M. R. and Stolper E. M. (1993) Noble gas solubilities in silicate melts and glasses: New experimental results for argon and the relationship between solubility and ionic porosity. *Geochim. Cosmochim. Acta* **57,** 5039–5051.

Cartigny P., Boyd S. R., Harris J. W., and Javoy M. (1997) Nitrogen isotopes in diamonds from Fuxian, China: The mantle signature. *Terra Nova* **9,** 175–179.

Cartigny P., Harris J. W., and Javoy M. (1998) Subduction-related diamonds? The evidence for a mantle-derived origin from coupled $\delta^{13}C$-$\delta^{15}N$ determinations. *Chem. Geol.* **147,** 147–159.

Cartigny P., Jendrzejewski F., Pineau F., Petit E., and Javoy M. (2001) Volatile (C, N, Ar) variability in MORB and the respective roles of mantle source heterogeneity and degassing: the case of the Southwest Indian Ridge. *Earth Planet. Sci. Lett.* **194,** 241–257.

Chamorro E. M., Brooker R. A., Wartho J-A., Wood B. J., Kelly S. P., and Blundy J. D. (2002) Ar and K partitioning between clinopyroxene and silicate melt to 8 GPa. *Geochim. Cosmochim. Acta* **66,** 507–519.

Chamorro-Pérez E., Gillet P., and Jambon A. (1996) Argon solubility in silicate melts at very high pressures. Experimental set-up and preliminary results for anorthite and silicate melts. *Earth Planet. Sci. Lett.* **145,** 97–107.

Chamorro-Pérez E., Gillet P., Jambon A., Bardo J., and McMillan P. (1998) Low argon solubility in silicate melts at high pressure. *Nature* **393,** 352–355.

Chou C. L., Shaw D. M., and Crocket J. H. (1983) Siderophile trace elements in the Earth's oceanic crust and upper mantle. *J. Geophys. Res.* **88, (***Suppl.***)**, A507–A518.

Christie D. M., Carmichael I. S. E., and Langmuir C. H. (1986) Oxidation states of mid-ocean ridge basalt glasses. *Earth Planet. Sci. Lett.* **79,** 397–411.

Fogel R. A. (1994) Nitrogen solubility in aubrite and E chondrite melts. *Lunar Planet. Sci. Conf.* **25,** 383–384.

Frischat G. H., Buschmann O., and Meyer H. (1978) Diffusion of nitrogen in glass melts. *Glastechn. Ber.* **51,** 321–327.

Gomersall D. W., McLean A. and Ward R. G. (1968) *Trans. Met. Soc. AIME* **242,** 1309–1315.

Haendel D., Muhle K., Nitzsche H., Stiehl G., and Wand U. (1986) Isotopic variations of the fixed nitrogen in metamorphic rocks. *Geochim. Cosmochim. Acta* **50,** 749–758.

Hashizume K. and Sugiura N. (1990) Precise measurement of nitrogen isotopic composition using a quadrupole mass spectrometer. *Mass Spectrosc.* **38,** 269–286.

Hayatsu A. and Waboso C. E. (1985) The solubility of rare gases in silicate melts and implications for K-Ar dating. *Chem. Geol.* **52,** 97–102.

Hiyagon H. and Ozima M. (1986) Partition og noble gases between olivine and basalt melt. *Geochim. Cosmochim. Acta* **50,** 2045–2057.

Hiyagon H., Ozima M., Marty B., Zashu S., and Sakai H. (1992) Noble gases in submarine glasses from mid-oceanic ridges and Loihi seamount: Constraints on early history of the Earth. *Geochim. Cosmochim. Acta* **56,** 1301–1316.

Humbert F (1998) *Solubilité de l'Azote Dans les Silicates Liquids*. Ph.D. dissertation, Université Henri Poincaré, Nancy, France.

Ito K. and Fruehan R. J. (1988) Thermodynamics of nitrogen in CaO-SiO_2-Al_2O_3 slags and its reaction with Fe-C_{sat}. *Melts Metall. Trans. B* **19B,** 419–425.

Jagoutz E., Palme H., Baddenhausen H., Blum K., Cendales M., Dreibus G., Spettel B., Lorenz V., and Wänke H. (1979) The abundance of major, minor and trace elements in the Earth's mantle as derived from primitive ultramafic nodules. *Proc. Lunar Planet. Sci. Conf.* **10,** 2031–2050.

Jambon A., Weber H., and Braun O. (1986) Solubility of He, Ne, Ar, Kr and Xe in a basalt melt in the range 1250–1600°C: Geochemical implications. *Geochim. Cosmochim. Acta* **50,** 401–408.

Javoy M. (1998) The birth of the Earth's atmosphere: The behaviour and fate of its major elements. *Chem. Geol.* **147,** 11–25.

Javoy M. and Pineau F. (1991) The volatile record of a popping rock from the Mid-Atlantic Ridge at 14°N: Chemical and isotopic composition of gases trapped in the vesicules. *Earth Planet. Sci. Lett.* **107,** 598–611.

Javoy M., Pineau F., and Demaiffe D. (1984) Nitrogen and carbon isotopic composition in the diamonds of Mbuji Mayi (Zaïre). *Earth Planet. Sci. Lett.* **68,** 399–422.

Jones J. H. and Drake M. J. (1986) Geochemical constraints on core formation in the Earth. *Nature* **322,** 221–228.

Kargel J. S. and Lewis J. S. (1993) The composition and early evolution of the Earth. *Icarus* **105,** 1–25.

Kasamatsu Y. and Matoba S. (1959) Activitiy of nitrogen in liquid pure iron. *Tetsu-to Hagane* **45,** 22–27.

Kelly S. (2002) Excess argon in K-Ar and Ar-Ar geochronology. *Chem. Geol.* **188,** 1–22.

Kesson S. E. and Holloway J. R. (1974) The generation of N_2-CO_2-H_2O fluids for use in hydrothermal experimentation II. Melting of albite in a multispecies fluid. *Am. Mineral.* **59,** 598–603.

Kirsten T. (1968) Incorporation of rare gases in solidifying enstatite melts. *J. Geophys. Res.* **73,** 2807–2810.

Kuno H. (1935) Preliminary note on the occurrence of pigeonite as phenocrysts in some pyroxene-andesite from Hakone volcano. *J. Geol. Soc.* **42,** 39–44.

Kuramoto K. and Matsui T. (1996) Partitioning of H and C between the mantle and core during the core formation in the Earth: Its implications for the atmospheric evolution and redox state of early mantle. *J. Geophys. Res.* **101,** 14909–14932.

Lux G. (1987) The behavior of noble gases in silicate liquids: Solution, diffusion, bubbles and surface effects, with application to natural samples. *Geochim. Cosmochim. Acta* **51,** 1549–1560.

Martinez E. R. and Sano N. (1990) Nitrogen solubility in CaO-SiO_2, CaO-MgO-SiO_2, and BaO-MgO-SiO_2 melts. *Metall. Trans. B* **21B,** 97–104.

Marty B. (1995) Nitrogen content of the mantle inferred from N_2-Ar correlation in oceanic basalts. *Nature* **377,** 326–329.

Marty B. and Zimmermann L. (1999) Volatiles (He, C, N, Ar) in mid-ocean ridge basalts: Assessment of shallow-level fractionation and characterization of source composition. *Geochim. Cosmochim. Acta* **63,** 3619–3633.

Marty B., Lenoble M., and Vassard N. (1995) Nitrogen, helium and argon in basalt: A static mass spectrometric study. *Chem. Geol.* **120,** 183–195.

Marty B., Zimmermann L., and Humbert F. (1996) Nitrogen isotopic composition of the silicate Earth and its bearing on Earth-atmosphere evolution. *Lunar Planet. Sci.* **27,** 819–820.

Matsuda J., Sudo M., Ozima M., Ito K., Ohtaka O., and Ito E. (1993) Noble gas partitioning between metal and silicate under high pressures. *Science* **259,** 788–790.

Miyagi I. (1995) Re-examination of water solubility in albite melt. *Proc. Jpn. Acad. B* **71,** 121–125.

Miyazaki A (1996) *Studies on Solubilities of Nitrogen and Noble Gases in Silicate Melts.* Ph.D. dissertation, University of Tokyo.

Miyazaki A., Hiyagon H., and Sugiura N. (1995) Solubilities of nitrogen and argon in basalt melt under oxidizing conditions. In *Volatiles in Earth and Solar System* (ed. K. A. Farley), pp. 276–283. AIP, New York.

Montana A., Guo Q., Boettcher S., White B. S., and Brearley M. (1993) Xe and Ar in high-pressure silicate liquids. *Am. Mineral.* **78,** 1135–1142.

Moore W. J. (1962) In *Physical Chemistry*. 3rd ed. Prentice Hall, Englewood Cliffs, NJ.

Mysen B. O. (1986) Structure and petrologically important properties of silicate melts relevant to natural magmatic liquids. In *MAC Short Course, Vol. 12: Silicate Melts: Their Properties and Structure Applied to Problems in Geochemistry, Petrology, Economic Geology and Planetary Geology* (ed. C. M. Scarfe), pp. 180–209. Mineralogical Association of Canada.

Nadeau S., Pineau F., Javoy M., and Francis D. (1990) Carbon concentrations and isotopic ratios in fluid-inclusion-bearing upper-mantle xenoliths along the northwestern margin of North America. *Chem. Geol.* **81,** 271–297.

Nishio Y., Ishii T., Gamo T., and Sano Y. (1999) Volatile element isotopic systematics of the Rodrigues Triple Junction Indian Ocean MORB: Implications for mantle heterogeneity. *Earth Planet. Sci. Lett.* **170,** 21–253.

Norris T. L. and Schaeffer O. A. (1982) Total nitrogen content of deep sea basalt. *Geochim. Cosmochim. Acta* **46,** 371–379.

Ono H., Morita K., and Sano N. (1997) Kinetic studies on the dissolution of nitrogen in CaO-Al_2O3, CaO-SiO2, and CaO-CaF2 melts. *Metall. Trans. B* **28B,** 633–638.

Peters K. E., Sweeney R. E., and Kaplan I. R. (1978) Correlation of carbon and nitrogen stable isotope ratios in sedimentary organic matter. *Limnol. Oceanogr.* **23,** 598–604.

Pinti D. L. and Hashizume K. (2001) ^{15}N-depleted nitrogen in Early Archean kerogens: Clues on ancient marine chemosynthetic-based ecosystems? A comment to Beaumont, V., Robert, F., 1999. Precambrian Res. 96, 63–82. *Precam. Res.* **105,** 85–88.

Ryall W. R. and Muan A. (1969) Silicon oxinitride stability. *Science* **165,** 1363–1364.

Schmidt B. C. and Keppler H. (2002) Experimental evidence for high noble gas solubilities in silicate melts under mantle pressures. *Earth Planet. Sci. Lett.* **195,** 277–290.

Shibata T., Takahashi E., and Ozima M. (1994) Noble gas partition between basaltic melt and olivine crystals at high pressures. In *Noble Gas Geochemistry and Cosmochemistry* (ed. J. Matsuda), pp. 343–354. Terra Scientific Publishing Company, Tokyo, Japan.

Shibata T., Takahashi E., and Matsuda J. (1996) Noble gas solubility in binary CaO-SiO_2 system. *Geophys. Res. Lett.* **23,** 3139–3142.

Shibata T., Takahashi E., and Matsuda J. (1998) Solubility of neon, argon, krypton, and xenon in binary and ternary silicate systems. *Geochim. Cosmochim. Acta* **62,** 1241–1253.

Shimoo T., Kimura H., and Kawai M. (1972) Study of nitrogen in liquid CaO-Al_2O_3 and CaO-SiO_2-Al_2O_3 in the graphite cruicible. *J. Jpn. Inst. Met.* **35,** 1103–1108.

Sun S. S. (1982) Chemical composition and origin of the Earth's primitive mantle. *Geochim. Cosmochim. Acta* **46,** 179–192.

Tolstikhin I. N. and Marty B. (1998) The evolution of terrestrial volatiles: A view from helium, neon, argon and nitrogen isotope modeling. *Chem. Geol.* **147,** 27–52.

Tsukihashi F., Matsumoto F., Hyodo T., Yukinobu M., and Sano N. (1985) Phosphorus and manganese distribution between carbon-saturated iron and Na_2O-SiO_2 melts and nitrogen solubility in the melts. *Tetsu-to Hagane* **71,** 823–830.

White B. S., Bearley M., and Montana A. (1989) Solubility of argon in silicate liquids at high pressures. *Am. Mineral.* **74,** 513–529.

Wood B. J. and Virgo D. (1989) Upper mantle oxidation state: Ferric iron contents of lherzolite spinels by ^{57}Fe Mössbauer spectroscopy and resultant oxygen fugacities. *Geochem. Cosmochim. Acta* **53,** 1277–1291.

Zhang Y. and Zindler A. (1993) Distribution and evolution of carbon and nitrogen in Earth. *Earth Planet. Sci. Lett.* **117,** 331–345

APPENDIX

Table A1. Analytical data of nitrogen and noble gases (atmospheric pressure experiments).

Sample (weight)	Temp. (°C)	Extraction method	Nitrogen (mol/g)			$Ex^{15}N^{15}N$ (mol/g), E-12	^{40}Ar (mol/g), E-12	^{20}Ne (mol/g), E-12
			$^{14}N^{14}N$, E-9	$^{14}N^{15}N$, E-12	$^{15}N^{15}N$, E-15			
L-14	400	RF	8.880	63.23	112.78	0.118	0.04	0.10
(0.05502 g)	600	RF	4.410	31.80	57.33	0.182	0.00	0.10
	800	RF	1.560	11.87	22.62	0.354	6.71	0.16
	1000	RF	0.827	6.63	13.31	0.365	8.45	0.47
	1200	RF	1.830	20.50	57.65	3.906	79.50	1.36
	1200	RF	0.145	1.07	1.97	0.024	1.25	1.36
	1100	L	0.718	5.11	9.12	0.007	0.90	0.00
	1600	L	0.329	2.38	4.31	0.014	1.12	0.00
	1700	L	0.371	2.67	4.82	0.011	0.58	0.00
	Sum					4.674	97.61	3.55
L-15	400	RF	2.130	15.02	26.41	0.060	0.31	1.30
(0.09388 g)	600	RF	0.932	6.70	12.02	0.665	0.16	1.44
	800	RF	0.244	1.84	3.49	0.513	7.02	2.67

(Continued)

Table A1. (Continued)

Sample (weight)	Temp. (°C)	Extraction method	Nitrogen (mol/g)			$Ex^{15}N^{15}N$ (mol/g), E-12	^{40}Ar (mol/g), E-12	^{20}Ne (mol/g), E-12
			$^{14}N^{14}N$, E-9	$^{14}N^{15}N$, E-12	$^{15}N^{15}N$, E-15			
	1000	RF	0.250	1.99	3.93	1.009	13.30	0.00
	1200	RF	0.185	2.41	7.81	5.918	97.10	0.00
	1200	RF	0.032	0.23	0.43	0.056	0.48	0.00
	1100	L	0.029	0.21	0.37	0.000	0.27	0.013
	1600	L	0.052	0.37	0.67	0.000	0.57	0.01
	1700	L	0.010	0.07	0.13	0.001	0.31	0.01
	Sum					7.497	118.94	5.45
L-16	400	RF	17.900	124.23	214.80	0.000	0.69	1.56
(0.06375 g)	600	RF	6.180	44.43	79.72	0.210	0.46	1.72
	800	RF	3.190	24.21	45.94	0.726	9.70	2.83
	1000	RF	0.991	8.23	17.05	0.602	9.32	0.00
	1200	RF	1.910	26.74	94.16	7.588	123.00	0.00
	1200	RF	0.517	3.85	7.19	0.104	1.60	0.00
	1100	L	0.078	0.56	1.01	0.002	0.32	0.02
	1600	L	0.393	3.01	5.78	0.100	2.16	0.02
	1700	L	0.127	1.13	2.55	0.118	3.12	0.02
	Sum					9.238	149.36	6.17
L-17	400	RF	5.500	39.16	69.85	0.000	0.47	0.74
(0.05638 g)	600	RF	1.030	7.53	13.80	0.077	0.00	0.96
	800	RF	1.250	9.09	16.50	0.672	0.00	1.14
	1000	RF	1.260	9.25	17.01	0.125	0.98	0.87
	1200	RF	0.965	13.32	45.93	6.891	106.00	2.31
	1200	RF	0.000	0.00	0.00	0.028	0.00	0.00
	1100	L	0.131	0.95	1.73	0.006	0.96	0.02
	1600	L	0.515	3.94	7.57	0.125	2.83	0.02
	1700	L	0.270	2.15	4.29	0.108	2.55	0.02
	Sum					7.949	112.36	6.07
L-18	400	RF	0.274	2.04	3.78	0.037	0.00	0.39
(0.06264 g)	600	RF	0.480	3.53	6.48	0.045	0.19	1.44
	800	RF	0.565	4.27	8.08	0.115	3.22	2.88
	1000	RF	0.870	6.65	12.70	0.211	3.75	0.90
	1200	RF	1.940	26.19	88.85	6.476	125.00	1.13
	1200	RF	0.000	0.00	0.00	0.023	0.00	0.33
		CR	0.050	0.75	2.83	0.200	7.70	0.00
	1100	L	1.060	7.60	13.57	0.000	0.13	0.00
	1600	L	5.240	38.04	69.17	0.392	17.00	0.01
	1700	L	1.290	10.02	19.48	0.491	10.10	0.02
	Sum					7.907	166.96	7.10
L-19	400	RF	0.092	0.67	1.23	0.008	0.00	0.02
(0.04107 g)	600	RF	0.124	0.90	1.65	0.009	0.44	0.78
	800	RF	0.076	0.56	1.03	0.010	0.98	2.06
	1000	RF	0.070	0.55	1.08	0.027	3.21	1.21
	1200	RF	1.170	13.69	39.66	2.716	136.00	2.32
	1200	RF	0.112	0.82	1.49	0.010	7.14	2.12
		CR	0.005	0.05	0.15	0.009	2.52	0.00
	1100	L	0.258	1.82	3.23	0.000	0.51	0.00
	1600	L	7.650	55.00	98.69	0.226	16.00	0.01
	1700	L	0.374	2.91	5.68	0.148	8.37	0.01
	1800	L	0.151	1.08	1.95	0.008	1.74	0.02
	Sum					3.153	176.39	8.55

Gas extraction method: CR = crushing, RF = combustion with the resistance furnace, L = combustion with the laser irradiation.

Table A2. Analytical data of nitrogen and argon (high pressure experiments).

	H-9 (0.00775 g)		H-10-1 (0.01382 g)		H-10-2 (0.00716 g)		H-10-3 (0.00834 g)		H-10-4 (0.01861 g)		H-10-5 (0.03062 g)	
Temp. (°C)	$^{14}N^{14}N$	^{40}Ar	$^{14}N^{14}N$	^{40}Ar	$^{14}N^{14}N$	^{40}Ar	$^{14}N^{14}N$	^{40}Ar	$^{14}N^{14}N$	^{40}Ar	$^{14}N^{14}N$	^{40}Ar
	10^{-6} (mol/g)		10^{-6} (mol/g)		10^{-6} (mol/g)		10^{-6} (mol/g)		10^{-6} (mol/g)		10^{-6} (mol/g)	
Cr#1	6.24E-05	0.004	1.35E-04	3.59E-03	2.93E-04	1.27E-03	2.34E-05	3.00E-03	1.86E-05	1.77E-03	5.28E-03	0.025
Cr#2	6.06E-06	8.51E-04	9.66E-07	9.65E-05	7.54E-05	2.89E-04	1.28E-05	3.37E-04	9.62E-07	1.43E-04	3.64E-05	0.002
400	0.038	0.002	0.034	0.001	0.004	0.000	0.004	0.001	0.001	0.001	0.0078	0.000
500	0.113	0.010	0.004	0.002	0.006	0.001	0.005	0.003	0.002	0.002	0.0064	0.000
600	0.017	0.048	0.008	0.011	0.013	0.004	0.006	0.009	0.001	0.003	0.0184	0.000
700	0.029	0.171	0.009	0.043	0.009	0.008	0.003	0.011	0.002	0.008	0.0071	0.001
800	0.192	1.490	0.117	1.150	0.111	0.480	0.028	0.232	0.050	0.446	0.0037	0.022
900	0.401	4.040	0.298	1.650	0.141	0.745	0.082	0.662	0.113	0.913	0.0055	0.059
1000	0.455	4.130	0.328	3.330	0.306	1.490	0.497	4.980	0.155	0.919	0.0017	0.017
1100	0.025	0.160	0.066	0.553	0.445	2.460	0.068	0.650	0.418	2.580	0.0603	0.762
1200	0.024	0.164	0.053	0.366	0.065	0.320	0.031	0.246	0.038	0.333	0.0036	0.014
1200					0.003	0.006	0.001	0.001	0.000	0.000	0.0015	0.006
1200											0.0012	0.004
1200											0.0014	0.007
Sum	1.142	10.203	0.880	7.103	1.079	5.514	0.716	6.791	0.777	5.202	0.0788	0.891

Cr# = crushing.